

# Redundant and scattered genetic determinants for coumarin biodegradation in *Pseudomonas* sp. strain NyZ480

Yichao Gu,<sup>1,2</sup> Tao Li,<sup>1,2</sup> Ning-Yi Zhou<sup>1,2</sup>

**AUTHOR AFFILIATIONS** See affiliation list on p. 19.

**ABSTRACT** Coumarin (COU) is both a naturally derived phytotoxin and a synthetic pollutant which causes hepatotoxicity in susceptible humans. Microbes have potentials in COU biodegradation; however, its underlying genetic determinants remain unknown. *Pseudomonas* sp. strain NyZ480, a robust COU degrader, has been isolated and proven to grow on COU as its sole carbon source. In this study, five homologs of xenobiotic reductase A scattered throughout the chromosome of strain NyZ480 were identified, which catalyzed the conversion of COU to dihydrocoumarin (DHC) *in vitro*. Phylogenetic analysis indicated that these COU reductases belong to different subgroups of the old yellow enzyme family. Moreover, two hydrolases (CouB1 and CouB2) homologous to the 3,4-dihydrocoumarin hydrolase in the fluorene degradation were found to accelerate the generation of melilotic acid (MA) from DHC. CouC, a new member from the group A flavin monooxygenase, was heterologously expressed and purified, catalyzing the hydroxylation of MA to produce 3-(2,3-dihydroxyphenyl)propionate (DHPP). Gene deletion and complementation of *couC* indicated that *couC* played an essential role in the COU catabolism in strain NyZ480, considering that the genes involved in the downstream catabolism of DHPP have been characterized (Y. Xu and N. Y. Zhou, *Appl Environ Microbiol* 86:e02385-19, 2020) and homologous catabolic cluster exists in strain NyZ480. This study elucidated the genetic determinants for complete degradation of COU by *Pseudomonas* sp. strain NyZ480.

**IMPORTANCE** Coumarin (COU) is a phytochemical widely distributed in the plant kingdom and also artificially produced as an ingredient for personal care products. Hence, the environmental occurrence of COU has been reported in different places. Toxicologically, COU was proven hepatotoxic to individuals with mutations in the CYP2A6 gene and listed as a group 3 carcinogen by the International Agency for Research on Cancer and thus has raised increasing concerns. Until now, different physicochemical methods have been developed for the removal of COU, whereas their practical applications were hampered due to high cost and the risk of secondary contamination. In this study, genetic evidence and biochemical characterization of the COU degradation by *Pseudomonas* sp. strain NyZ480 are presented. With the gene and strain resources provided here, better managements of the hazards that humans face from COU could be achieved, and the possible microbiota-plant interaction mediated by the COU-utilizing rhizobacteria could also be investigated.

**KEYWORDS** biodegradation, coumarin, genetic redundancy, *Pseudomonas* sp. strain NyZ480

Rhizospheric exudation is of great significance to both plants and the associated root microbiome. For instance, nicotinic, shikimic, salicylic, and cinnamic compounds exuded by plants were evidenced to facilitate the microbial community assembly in rhizosphere (1); triterpenes were identified as plant-specialized metabolites which vastly

**Editor** Jeremy D. Semrau, University of Michigan-Ann Arbor, Ann Arbor, Michigan, USA

Address correspondence to Ning-Yi Zhou, ningyi.zhou@sjtu.edu.cn.

The authors declare no conflict of interest.

See the funding table on p. 19.

**Received** 30 June 2023

**Accepted** 18 August 2023

**Published** 10 October 2023

Copyright © 2023 American Society for Microbiology. All Rights Reserved.

contribute to the plant defense and signaling (2). Coumarin (COU, 1,2-benzopyrone), a chemical with a special odor, has been drawing increasing public attention, not only because of its important roles in plant physiology but also because of its potential hazards on humans. COU is produced in a wide range of plants including sweet clover (*Melilotus officinalis*), woodruff (*Asperula odorata*), cassia (*Cinnamomum cassia*), and lavender (*Lavandum officinalis*), etc. (3) As an allelopathic chemical (4), COU is biosynthesized and secreted by various plants so as to gain growth advantage and regulate the microbial community assembly (5, 6), subsequently leading to the presence and residue of COU in soil. In addition, COU easily diffuses in soil with rainfall and thus likely enters aquatic environment (7). Hence, the distribution of COU could be distributed throughout the ecosystem. In daily life, human exposure to COU is much more frequent than expected. Since COU-rich plants are often made into herbal medicines and spices (8, 9), consumption of these substances inevitably led to ingestion of COU (10, 11). Moreover, dermal contact with many personal care products also adds the exposure risk as artificially synthesized COU is often contained (12, 13). Due to its widely natural occurrence and anthropogenic sources, COU has been detected in rivers and groundwater in several cities (14–16); hence, it is listed as an emerging contaminant and gradually raises public concerns.

According to toxicological assessment, detrimental effects of COU have been recorded not only on experimental animals (17–19) but also in human clinical trials (20–22). Around the 1950s, it was firstly discovered that rat and dog suffered hepatotoxicity elicited by high-dose COU. Moreover, development of tumors was found in animals exposed to COU for long periods (23). As for humans, susceptibility to COU-induced hepatotoxicity was observed in a specific population (24). The reason underlying this phenomenon could be explained by the genetic polymorphism of CYP2A6 gene (25–27); its defective variants cause the production of toxic intermediates including coumarin 3,4-epoxide and *ortho*-hydroxyphenethyl aldehyde during the metabolism of COU in human body (28). Although the majority remains resistant to the hepatotoxicity of COU, the well-being of approximately 10% of the global population is still potentially impaired (28–34).

Lately, efforts have been made to address the COU contamination. Physicochemical approaches including UV-assisted electrochemical degradation (35), radical-dependent oxidation (36, 37), electro-Fenton, and subcritical water oxidation processes have been reported to be effective in treating COU (38), while their practical application is to some extent limited due to secondary contamination (39) and high cost. Microbial degradation of COU has also been studied (40–44), but no thorough molecular evidence was yet available. To elucidate its molecular mechanism and to provide genetic and enzymatic resources for the treatment of COU, *Pseudomonas* sp. strain NyZ480, a robust COU degrader, was isolated from root soil sample in Sichuan province, China, and thoroughly characterized in our previous study (45). Intermediates including dihydrocoumarin (DHC), melilotic acid (MA), and 3-(2,3-dihydroxyphenyl)propionate (DHPP) were identified to be products of the upstream catabolic pathway, and homologs of the *mhp* gene cluster (46) were proposed to be involved in the downstream pathway of COU catabolism (Fig. 1).

In this study, genetic determinants were presented to fill in the gap in COU degradation by *Pseudomonas* sp. strain NyZ480. Bioinformatic and biochemical analyses led to the identification of the genes involved in the first three biotransformation steps within the catabolic pathway. Specifically, several isozymes from the old yellow enzyme (OYE) family were shown to convert COU to DHC; two redundant hydrolases accelerated the ring fission of DHC to generate MA, a process that was shown to occur spontaneously at a slow rate; and a new member of the group A flavin-dependent monooxygenase was evidenced to be indispensable for the formation of DHPP from MA in strain NyZ480. In summation, this study provided an overall understanding of the COU biodegradation at the genetic and biochemical levels.

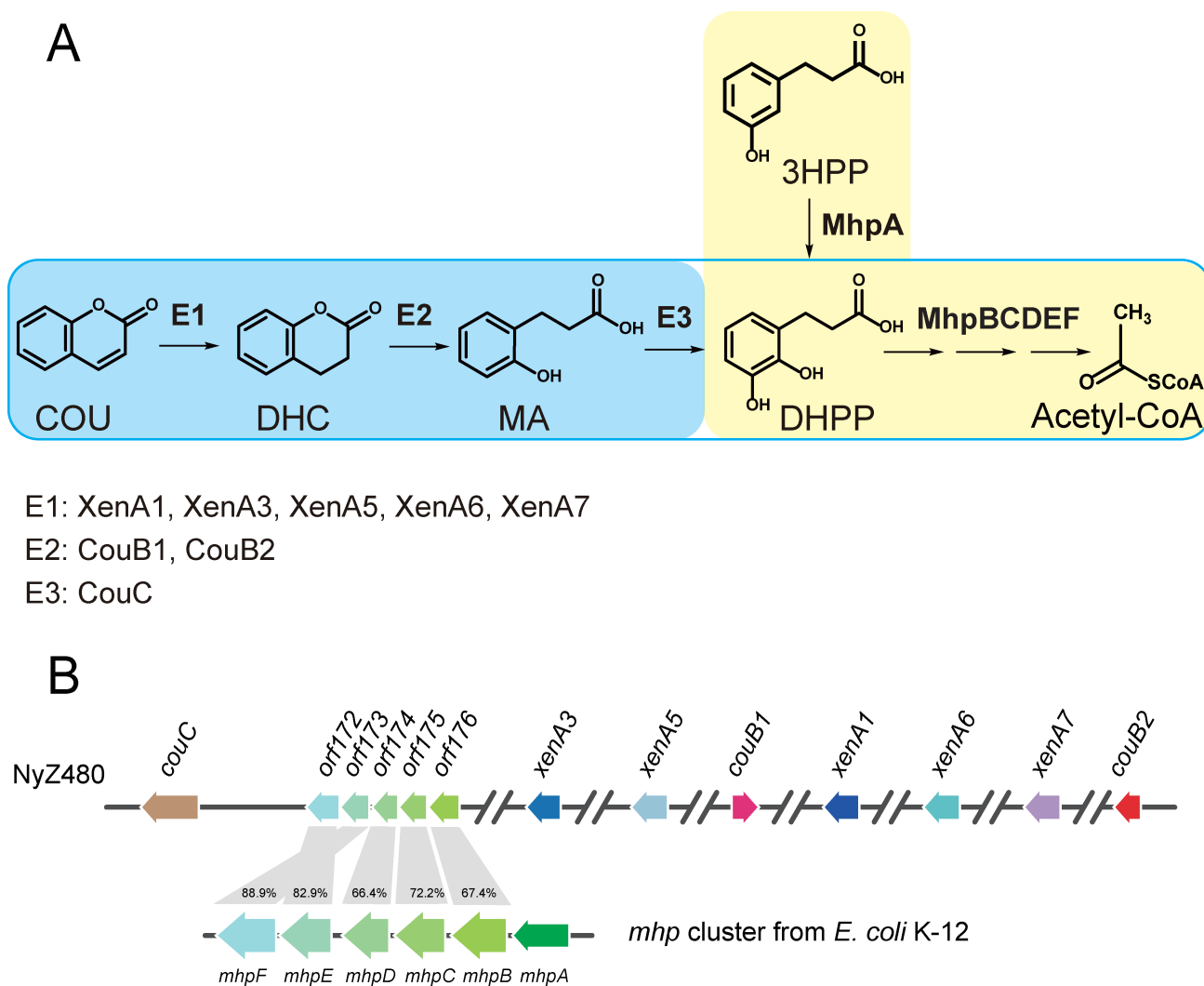


**FIG 1** Proposed catabolic pathway of COU in *Pseudomonas* sp. strain NyZ480 and the catabolic reactions catalyzed by respective gene products. (A) The COU upstream pathway is presented in the blue background; the 3HPP catabolic pathway in *E. coli* K-12 is shown in the yellow background. The complete COU catabolic pathway is indicated by the blue outline. The first two biotransformation steps might be catalyzed by enzymes other than the listed ones, and the conversion of DHC to MA could occur spontaneously. (B) Organization of the genes involved in the COU catabolism on the chromosome of *Pseudomonas* sp. strain NyZ480 and a comparison between the *mhp* cluster from *E. coli* K-12 (46) and the gene cluster including *orf172* to *orf176* from *Pseudomonas* sp. strain NyZ480. Abbreviations: COU, coumarin; DHC, dihydrocoumarin; MA, melilotic acid; 3HPP, 3-(2,3-dihydroxyphenyl)propionate; DHPP, 3-(2,3-dihydroxyphenyl)propionate.

## RESULTS

### Prediction of genes involved in the COU catabolism by genomic analysis

As discussed in our previous study, homologs of the *mhp* cluster for DHPP degradation in the 3-(2,3-dihydroxyphenyl)propionate (3HPP) catabolic pathway (46) were proposed to be involved in the downstream catabolism of COU in strain NyZ480 (45), as presented in Fig. 1. However, the genetic determinants for the conversion of COU to MA via DHC remained undiscovered. During the quinoline degradation by *Pseudomonas putida* 86, xenobiotic reductase A (XenA) was found capable of catalyzing the reduction of COU to generate DHC (47). Hence, XenA (accession number Q9R9V9) was used as query to search for possible homologs in the genome of strain NyZ480. As for the conversion of DHC to MA, the 3,4-dihydrocoumarin hydrolase (DCH; accession number Q83WC8) in *Arthrobacter* sp. strain F101 (48, 49), which catalyzes the identical transformation in the

fluorene degradation, was chosen as query. Above efforts led to the prediction of eight homologs of XenA and two homologs of DCH in strain NyZ480, as shown in Table 1.

### Strain NyZ480 harbors multiple genes converting COU to DHC

Gene *xenA1*, with the highest identity (93.7%) to *xenA*, was proposed the most likely to convert COU to DHC. Hence, *xenA1* was firstly inserted into pET-28a(+) and then introduced into *E. coli* BL21(DE3) cells for heterologous expression of recombinant XenA1. As shown in Fig. 2A, COU was gradually dissipated when being incubated with cells expressing XenA1. Meanwhile, two new peaks appeared on the high-performance liquid chromatography (HPLC) chromatogram, whose retention time was in consistent with those of the authentic DHC (16.2 min) and MA (12.6 min), respectively (Fig. 2B). Moreover, liquid chromatography-mass spectrometry (LC-MS) analysis indicated that the *m/z* values of these two products were 149.0594 and 165.0561 (Fig. 2C), identical to those of the authentic DHC and MA, respectively. Intriguingly, unlike the continuous accumulation of MA during this biotransformation, DHC is a transient intermediate (Fig. S1), which could be attributed to its spontaneous hydrolysis as observed in our previous study (45). Quantification data obtained from HPLC analysis indicated that the combined amount of generated DHC and MA was equivalent to the amount of COU consumed throughout the time course of whole cell biotransformation (Fig. 2A). Finally, the XenA1-resultant DHC from COU was completely converted to MA via spontaneous hydrolysis. However, mutant strain NyZ480Δ*xenA1* retained its capability to grow with COU as its sole carbon source (Fig. S2). Hence, other 7 homologs of XenA were also studied for their biochemical functions as above. Among them, XenA3, XenA5, XenA6, and XenA7 possessed the same catalytic ability as XenA1 (Fig. S3). Based on the whole cell biotransformation assay, the COU conversion rate of XenA1 was determined as 60.09 μM<sup>-1</sup> min<sup>-1</sup> g<sup>-1</sup> wet weight cells. In addition, the conversion rate of XenA3, XenA5, XenA6, and XenA7 toward COU was 18.39%, 0.91%, 8.41%, and 16.99%, respectively, compared to XenA1. Indeed, multiple functional COU reductases were found in strain NyZ480. However, it remains elusive which ones of them carry out the exact function *in vivo*. Moreover, enzymes without significant similarity to XenA might be involved in the reaction, which certainly requires further investigation in the future.

### CouB1 and CouB2 hydrolyze DHC *in vitro*

The functions of the predicted DCH homologs from strain NyZ480 in the hydrolysis of DHC were investigated by heterologous expression of CouB1 and CouB2. Although spontaneous hydrolysis of DHC was observed in enzyme-free control, crude enzymes containing either CouB1 or CouB2 drastically accelerated the transformation of DHC to form MA (Fig. 3). Cell extracts of *E. coli* carrying pET-28a(+) had no stimulation on the conversion of DHC to MA. Although both CouB1 and CouB2 were able to rapidly convert

TABLE 1 Candidate enzymes involved in the COU catabolism in strain NyZ480

Query	Hits	Identity	E-value
XenA <sup>a</sup> (Q9R9V9) <sup>c</sup>	XenA1 (WEZ87495.1)	93.664%	0
	XenA6 (WEZ87656.1)	45.304%	5.11E-99
	XenA3 (WEZ89587.1)	31.143%	3.33E-38
	XenA4 (WEZ90108.1)	29.706%	5.10E-34
	XenA8 (WEZ88390.1)	27.826%	1.19E-31
	XenA2 (WEZ89206.1)	29.607%	4.59E-31
	XenA7 (WEZ87916.1)	28.212%	3.81E-25
	XenA5 (WEZ90623.1)	27.606%	1.43E-22
DCH <sup>b</sup> (Q83WC8)	CouB1 (WEZ86871.1)	77.174%	0
	CouB2 (WEZ88550.1)	45.455%	2.90E-84

<sup>a</sup>XenA (47) is the xenobiotic reductase A, converting COU to DHC.

<sup>b</sup>DCH is the 3,4-dihydrocoumarin hydrolase (48), catalyzing the hydrolysis of DHC to generate MA.

<sup>c</sup>Accession numbers are indicated in the brackets.

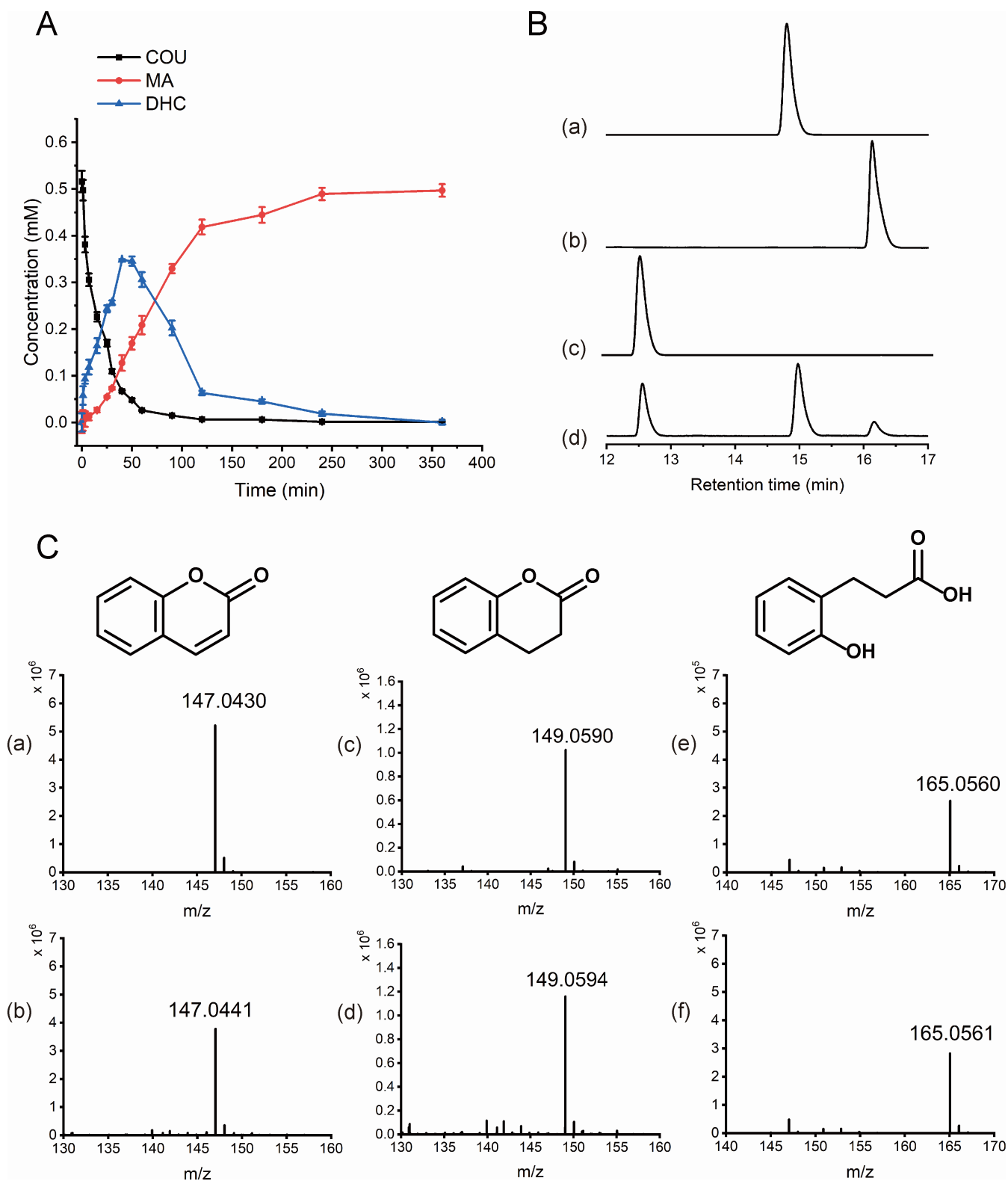


**FIG 2** Whole cell biotransformation of COU by *E. coli* pET-xenA1. (A) Time course of COU biotransformation by *E. coli* cells harboring pET-xenA1. Results are average values derived from the triplicated experiments, and standard deviations are plotted as error bars. (B) HPLC chromatograms of authentic COU (a), authentic DHC (b), authentic MA (c), and biotransformation products of COU catalyzed by cell suspension of *E. coli* pET-xenA1 (d). (C) Identification of the biotransformation products of COU by LC-MS. Mass spectra of authentic COU (a), authentic DHC (c), and authentic MA (e). Mass spectra of COU (b), DHC (d), and MA (f) captured during the biotransformation.

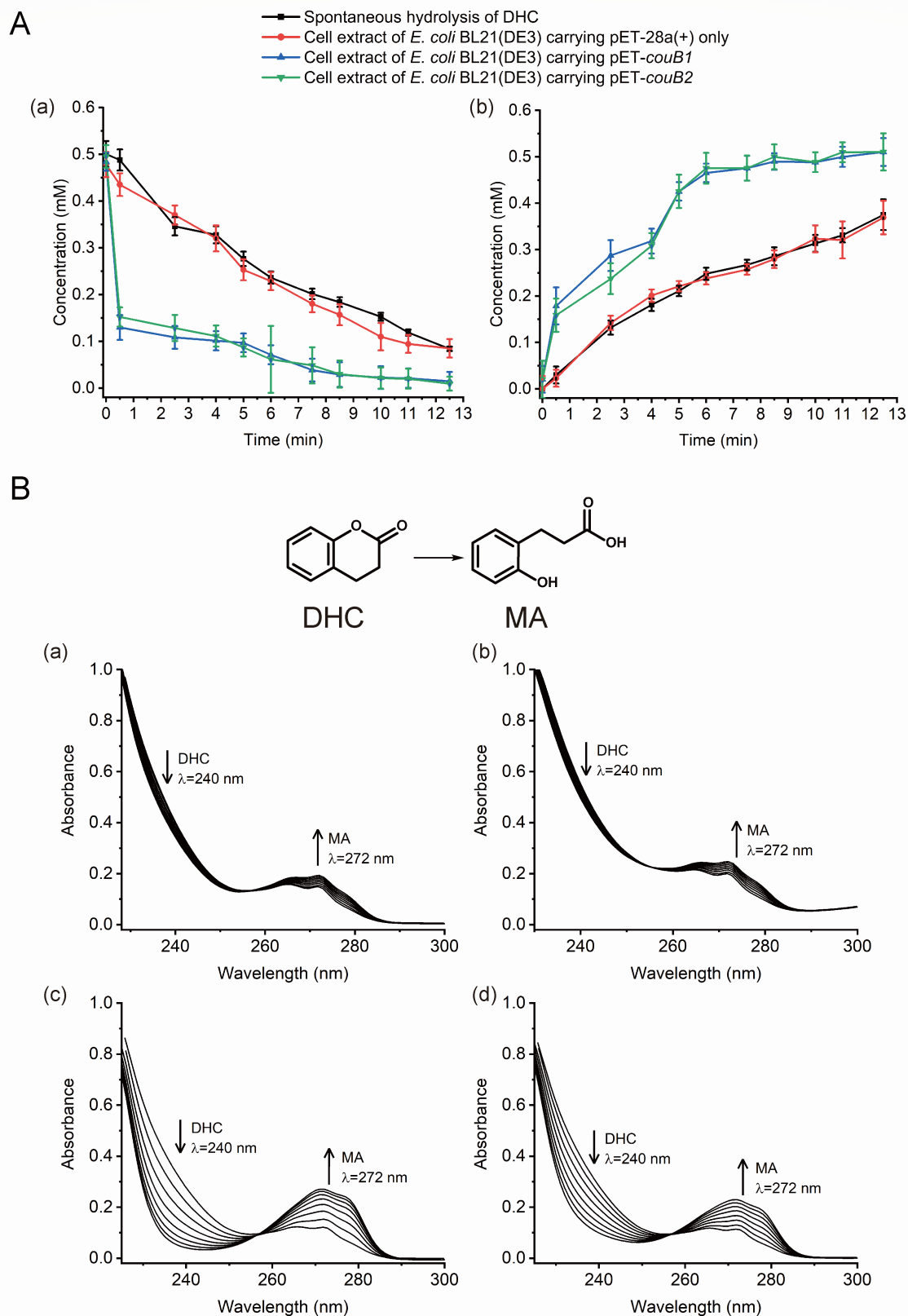


**FIG 3** CouB1 and CouB2 catalyze the hydrolysis of the lactone ring of DHC thus the formation of MA. (A) Time course of the conversion of DHC to MA quantified by HPLC analysis, decrease of DHC (a) and accumulation of MA (b) are presented separately. (B) UV spectrum scanning of DHC transformation in the enzyme-free Tris-HCl buffer (pH 8.0) (a), with the addition of cell extract prepared from *E. coli* harboring pET-28a(+) (b), pET-*couB1* (c), and pET-*couB2* (d), respectively. The spectra in panel B were recorded every 30 s.

DHC to MA, the specific activity of CouB1 ( $168.46 \pm 2.83$  U/mg) was 35-fold higher than that of CouB2 ( $4.85 \pm 0.14$  U/mg). Moreover, gene deletion was also conducted to verify the *in vivo* function of these two hydrolases. However, strains with either single or double deletion of *couB1* and *couB2* still grew on COU (Fig. S2).

### CouC catalyzes the hydroxylation of MA to generate DHPP

As mentioned in our previous study (45), the transcriptional level of the flavin adenine dinucleotide (FAD)-dependent monooxygenase encoding gene (*orf169*, designated *couC* here) that is 3.2 kb apart from the homologs of *mhp* gene cluster (involved in the catabolism of 3HPP to acetyl-CoA via DHPP) was upregulated ( $\log_2FC = 2.8$ ) by COU induction (Fig. 1B), and thus, CouC was hypothesized to catalyze the hydroxylation of MA to generate DHPP. Therefore, CouC was heterologously expressed and purified for its biochemical characterization. The approximate molecular mass of the recombinant His-tagged CouC was determined to be around 60 kDa by SDS-PAGE analysis (Fig. S4), close to the predicated value based on its amino acid sequence (63.9 kDa). UV spectrum scanning of MA transformation catalyzed by CouC showed a gradually decreased absorption at 340 nm (Fig. 4A), indicating the substrate-dependent consumption of cofactor NADH (no activity was detected with NADPH). The slight rise of the absorption peak at 275 nm was likely due to the formation of DHPP. The  $K_m$  and  $K_{cat}$  values of CouC for MA were determined to be  $2.54 \pm 0.42 \mu\text{M}^{-1} \text{min}^{-1}$  and  $7.86 \pm 0.19 \text{min}^{-1}$ , respectively. Moreover, the HPLC chromatogram captured during the catalysis of MA by CouC showed the decrease of MA (12.6 min) and the formation of a new product, whose retention time was identical to that of authentic DHPP (10.7 min) (Fig. 4B), and MA was stoichiometrically converted to DHPP by CouC, as shown in Fig. 4C. In addition, the formation of DHPP was also confirmed by LC-MS analysis through comparison with the authentic DHPP (Fig. 4D). In conclusion, the newly discovered CouC was determined as an NADH-dependent hydroxylase catalyzing the hydroxylation of MA to form DHPP in the catabolism of COU.

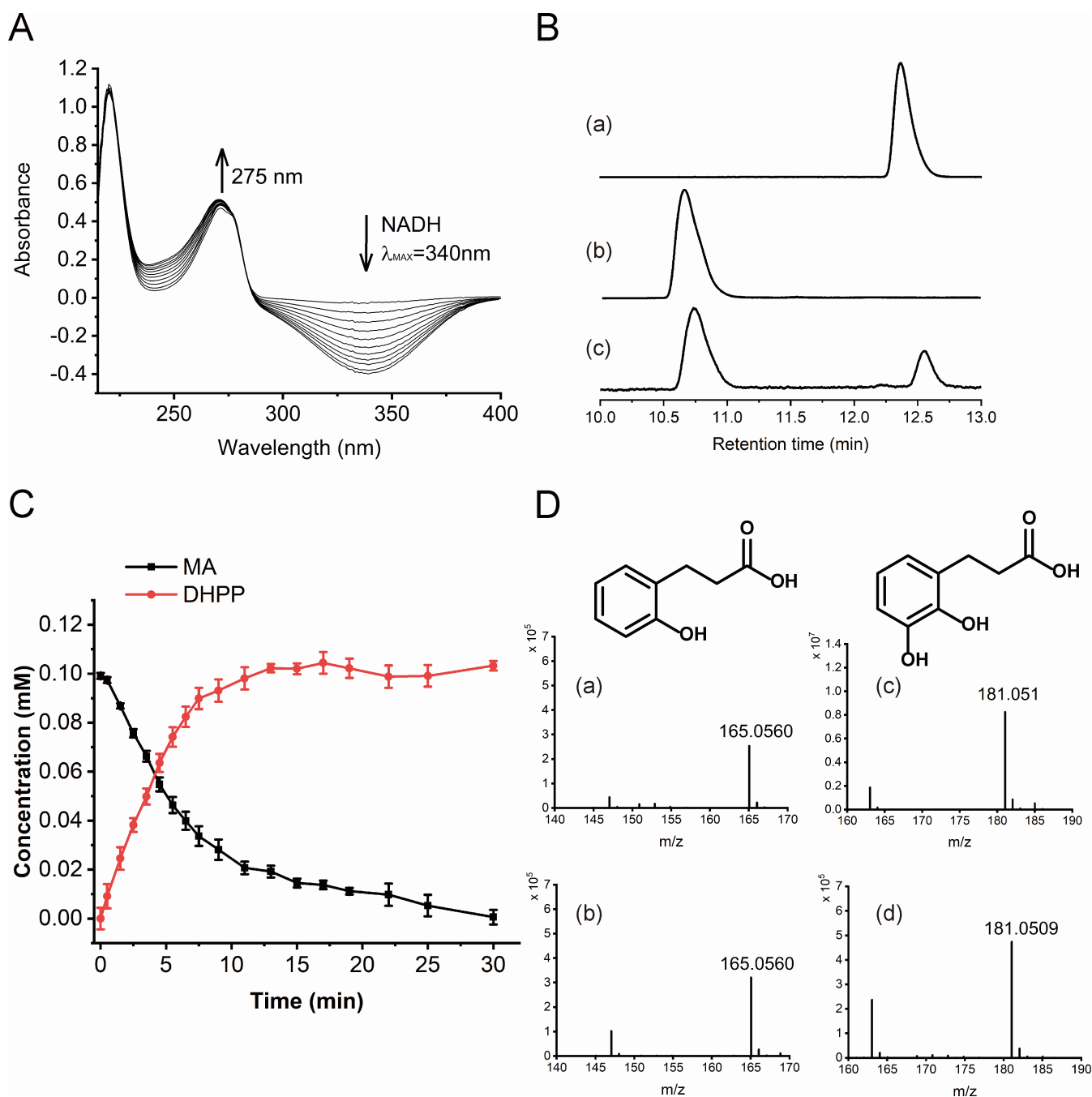
Gene deletion of *couC* was subsequently carried out to confirm its *in vivo* role in COU catabolism by strain NyZ480. The mutant strain NyZ480 $\Delta$ *couC* completely lost its ability to grow on COU as the sole carbon source, and gene *couC* complementation restored the mutant strain to its capability of utilizing COU for growth. Besides, strain NyZ480 $\Delta$ *couC* failed to grow on COU when containing the vector pBBRIMSC-2 only (Fig. 5). Overall, these results indicated that *couC* plays an essential role in the COU catabolism in strain NyZ480.

### Phylogenetic analysis of CouC

CouC was annotated as an FAD-dependent monooxygenase by KEGG database (Table S1). After further thorough analysis, DG and GD fingerprints, which are signature amino acid sequence motifs of the group A flavin monooxygenases (50), were identified in CouC. Hence, curated representatives of the group A flavin monooxygenases were selected for the phylogenetic analysis between CouC and these enzymes (Fig. 6). As it turned out, despite of the resemblance between MA and 3HPP in the overall chemical structure except for the difference in their hydroxyl position, CouC is distantly related to the MhpA-like hydroxylases of 3HPP. Instead, CouC is more closely related to phenol and dichlorophenol monooxygenases but seemingly forms a separate clade.

### Substrate specificity of CouC

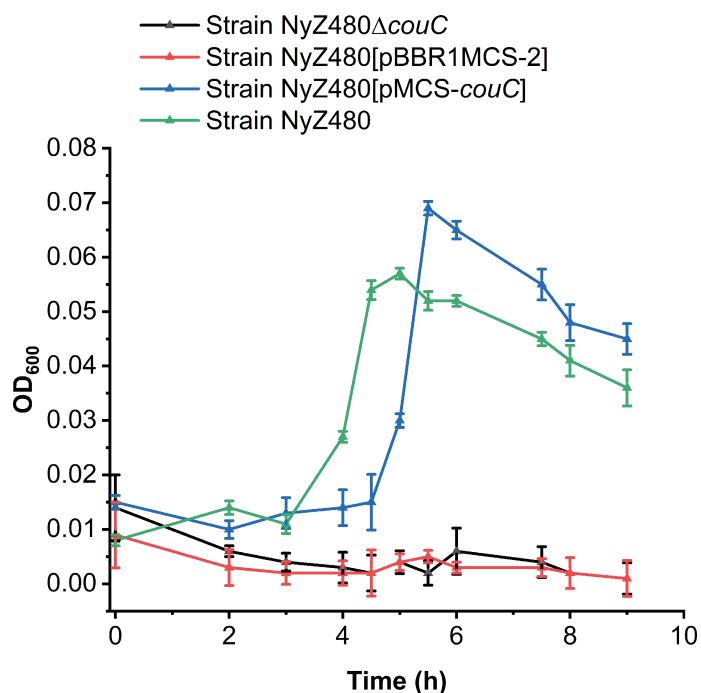
A number of substrates of group A flavin monooxygenases were used to study the catalytic specificity of CouC (Table 2). The specific activity of CouC toward MA was  $82.05 \pm 1.99$  U/mg, which was defined as 100%. Besides, CouC exhibited a low catalytic activity against *o*-coumaric acid, which probably could explain for our previous observation that strain NyZ480 was able to grow on *o*-coumaric acid yet at a slower rate compared with growing on COU (45). Moreover, CouC had weak hydroxylation activity



**FIG 4** Functional characterization of purified CouC. (A) UV spectrum scanning of MA transformation catalyzed by purified CouC. The spectra were recorded every 30 s, and the arrows indicate the trend of the spectral shifting. (B) HPLC chromatogram of MA standard (a), DHPP standard (b), and the reaction product derived from conversion of MA by CouC (c). (C) Time course of the hydroxylation of MA catalyzed by purified CouC, the consumption of MA, and the accumulation of DHPP were quantified via HPLC analysis. Results are average values derived from the triplicated experiments, and standard deviations are plotted as error bars. (D) Identification of the enzymatic products of MA by LC-MS. Mass spectra of authentic MA (a) and authentic DHPP (c); mass spectra of MA (b) and DHPP (d) captured during the enzyme assay.

against 3-hydroxycinnamic acid, 2-chlorophenol, cinnamic acid, 3-hydroxybenzoic acid, and 3HPP. However, 2,4-dichlorophenol was not a substrate for CouC, even though a close phylogenetic relationship between CouC and 2,4-dichlorophenol hydroxylases was observed.

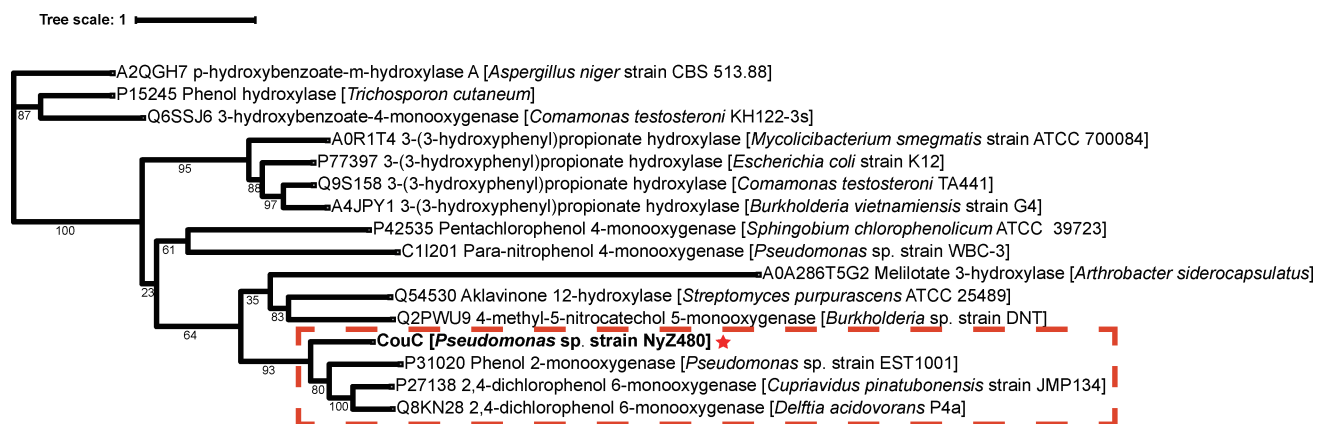




**FIG 5** Growth curves of wild-type strain NyZ480, *couC*-deleted strain NyZ480, and the complementary strains with COU as the sole carbon source. Strains were cultured in minimal medium supplemented with 0.5 mM COU as the sole carbon source on a rotary shaker (180 rpm, 30°C). All the results are average values derived from the triplicated experiments, and standard deviations are plotted as error bars. OD<sub>600</sub> is the optical density value measured at a wavelength of 600 nm.

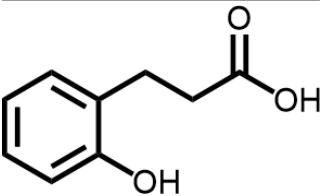
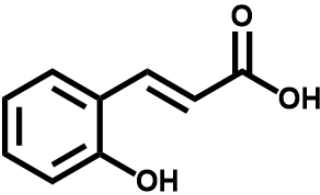
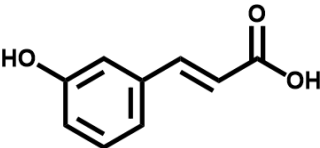
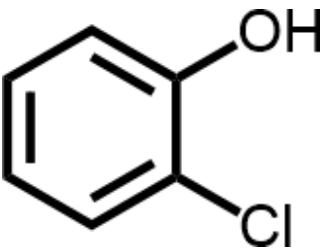
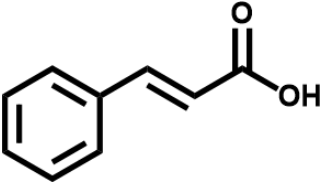
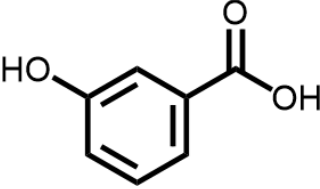
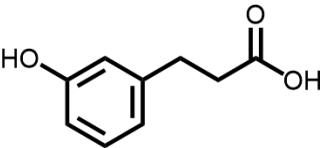
## DISCUSSION

This study thoroughly investigated the unreported genetic determinants for the microbial catabolism of COU. It was found that the first two biotransformation steps (from COU to MA via DHC) in the degradation pathway are likely executed by two sets of isoenzymes, whose encoding genes are dispersedly located on the chromosome of the COU utilizer strain NyZ480. Subsequently, a member from the group A flavin monooxygenases was newly identified here, which was evidenced to convert MA to DHPP. Combined with our previous conclusion that DHPP was further mineralized by the gene cluster comprising *orf172* to *orf176* in strain NyZ480 (45), the genetic determinants and biochemical identification of COU catabolism were elucidated in this study, which



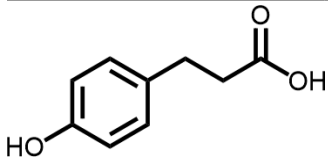
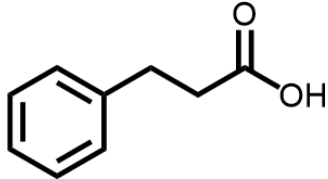
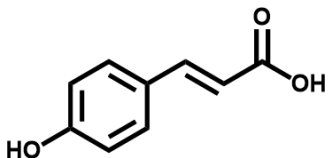
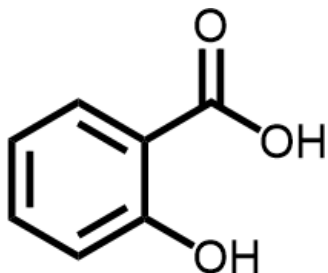
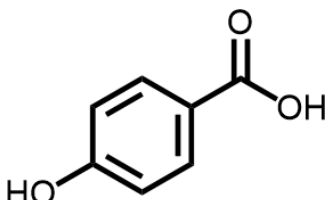
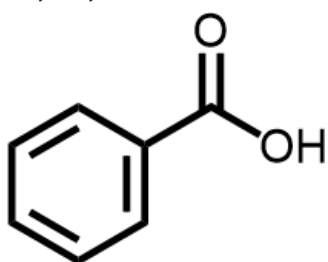
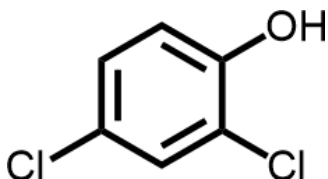
**FIG 6** Phylogenetic analysis of CouC (labeled with the red pentagram) illustrating its relationship to the curated representatives of the groups A flavin monooxygenases. Bootstrap values are shown on the branching nodes.

TABLE 2 Relative activities of CouC against different substrates<sup>a</sup>

Substrate	Relative activity
	100.0%
Melilotic acid	
	37.55%
<i>o</i> -Coumaric acid	
	6.40%
3-Hydroxycinnamic acid	
	0.16%
2-Chlorophenol	
	0.13%
Cinnamic acid	
	0.08%
3-Hydroxybenzoic acid	
	0.06%
3-(3-Hydroxyphenyl)propionate	

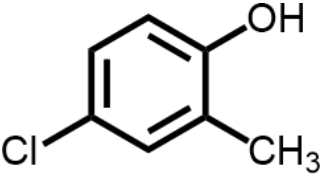
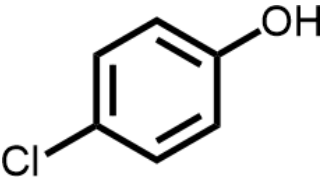
*(Continued on next page)*

TABLE 2 Relative activities of CouC against different substrates<sup>a</sup> (Continued)

Substrate	Relative activity
 3-(4-Hydroxyphenyl)propionate	ND <sup>b</sup>
 Hydrocinnamic acid	ND
 4-Hydroxycinnamic acid	ND
 Salicylic acid	ND
 4-Hydroxybenzoic acid	ND
 Benzoic acid	ND
 2,4-Dichlorophenol	ND

(Continued on next page)

TABLE 2 Relative activities of CouC against different substrates<sup>a</sup> (Continued)

Substrate	Relative activity
2,4-Dichlorophenol 	ND
4-Chloro-2-methylphenol 	ND
4-Chlorophenol	

<sup>a</sup>The relative activity of CouC against mellilotic acid was  $82.05 \pm 1.99 \text{ U mg}^{-1}$ , which was defined as 100%.

<sup>b</sup>ND, not detected.

deepened the perceptions on how bacteria recruit genes and enzymes from different existing pathways to assemble a new catabolic route for a plant-derived exudate.

It has long been recognized that genetic redundancy was prevalent in organisms, promoting robustness and adaptation to environmental stresses (51). Aromatic compounds of natural origin and anthropogenic sources are frequently detected in different environment and thus led to the evolution of diverse degradation capabilities in microorganisms. For instance, three redundant pathways catalyzing the catabolism of benzoate were identified in *Burkholderia xenovorans* LB400, which conferred a specific metabolic advantage to the strain (52). Two feruloyl-CoA synthase homologs were found in *Sagittula stellata* E-37, which played overlapping roles in the catabolism of hydroxycinnamate (53). Also, as reported in *Pigmentiphaga* sp. strain H8, three 4-hydroxybenzoate 3-hydroxylases (PHBH1–3) were identified, and the functionally redundant PHBH1 and PHBH2 not only catalyzed the transformation of 3-bromo-4-hydroxybenzoate but also assured the catabolic safety of 4-hydroxybenzoate by PHBH3 (54). In this study, COU reductase encoding genes *xenA1*, *xenA3*, *xenA5*, *xenA6*, and *xenA7*, dispersedly distributed homologs of *xenA* on the genome of strain NyZ480, were proven all active in the conversion of COU to DHC *in vitro*. This phenomenon of genetic redundancy might be attributed to the massive occurrences of COU and its analogs in soil (55, 56), where strain NyZ480 was isolated. Since COU and the so-called simple coumarins including scopoletin, fraxetin, esculetin, and sideretin, etc., are root exudates of various plants that possess antimicrobial activity (6, 57), soil microorganisms likely evolve an arsenal of tools to overcome the perturbation from these COU compounds. As the enzyme initializing the catabolism in strain NyZ480, COU reductases catalyze the reduction of unsaturated C=C bond of the lactone ring, thus resulting in the spontaneous ring fission of the resultant DHC. Intriguingly, simple coumarins all contain the same moiety of a lactone ring, which led us to assume that the redundant reductases could play pivotal roles in the microbial resistance to COU compounds as they likely initiate their degradation, thus preventing the potential harms. The versatile catabolic ability against the class of COU compounds in rhizobacteria could make possible impacts on their host plants. This assumption could be inferred from the instance where *Ralstonia solanacearum* enhances its virulence on tobacco through the degradation of the plant exudate salicylic acid (58).

Since the five functional COU reductases share various degrees of identity with XenA belonging to the OYE family (50), the phylogenetic relationship among these five COU reductases and several curated OYE representatives was investigated (Fig. 7). Intriguingly, the five functional enzymes are related to different subgroups of OYE: XenA1 and XenA6 belong to the Class II OYE, XenA3 and XenA5 belong to the Class Ia OYE, and

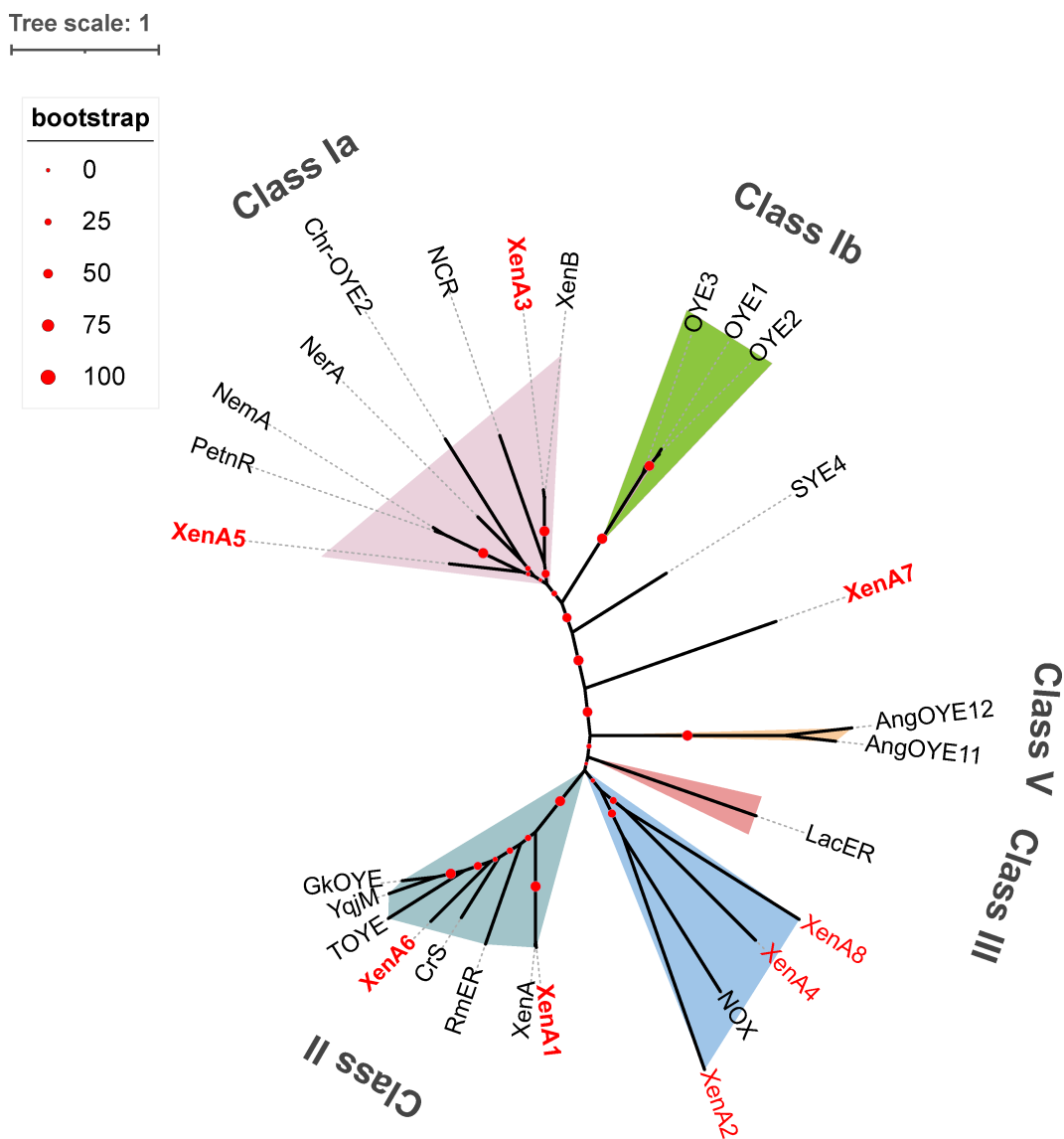


**FIG 7** Phylogenetic relationships between XenA1-8 and other enzymes from the OYE family. Accession numbers of the used sequences are listed in Table S2.

XenA7 separates itself from other OYEs to form an independent clade. Although the COU reductases are likely from different phylogenetic backgrounds (Fig. 7), they share conservative residues in the reactive pocket, namely, one histidine and one tyrosine at the corresponding site of XenA (Fig. 8A). As indicated by the deciphered crystalline structure of XenA (Fig. 8B; PDB entry 2H90), the histidine pair (His178 and His181) determines the binding of COU, and Tyr183 provides a hydride and a proton for the catalysis. Moreover, the His178 at the corresponding sites of the five functional COU reductases is all conserved, but the His181 at the corresponding sites of XenA3 and XenA5 is substituted by asparagine, even though they remain catalytic. As XenA1 shares 94% identity with XenA, its overall simulated structure and the COU-binding mode are almost identical to XenA (Fig. 8C). Although the other four COU reductases share relatively low identity with XenA, molecular docking prediction revealed that COU was fitted properly in the active sites in a similar conformation (Fig. S5), indicating that they shared a conserved mechanism for recognition and catalyzation of COU.

Redundant enzymatic catalysis was also observed in the hydrolysis of DHC to generate MA, even though this reaction could occur spontaneously *in vitro*. In addition,

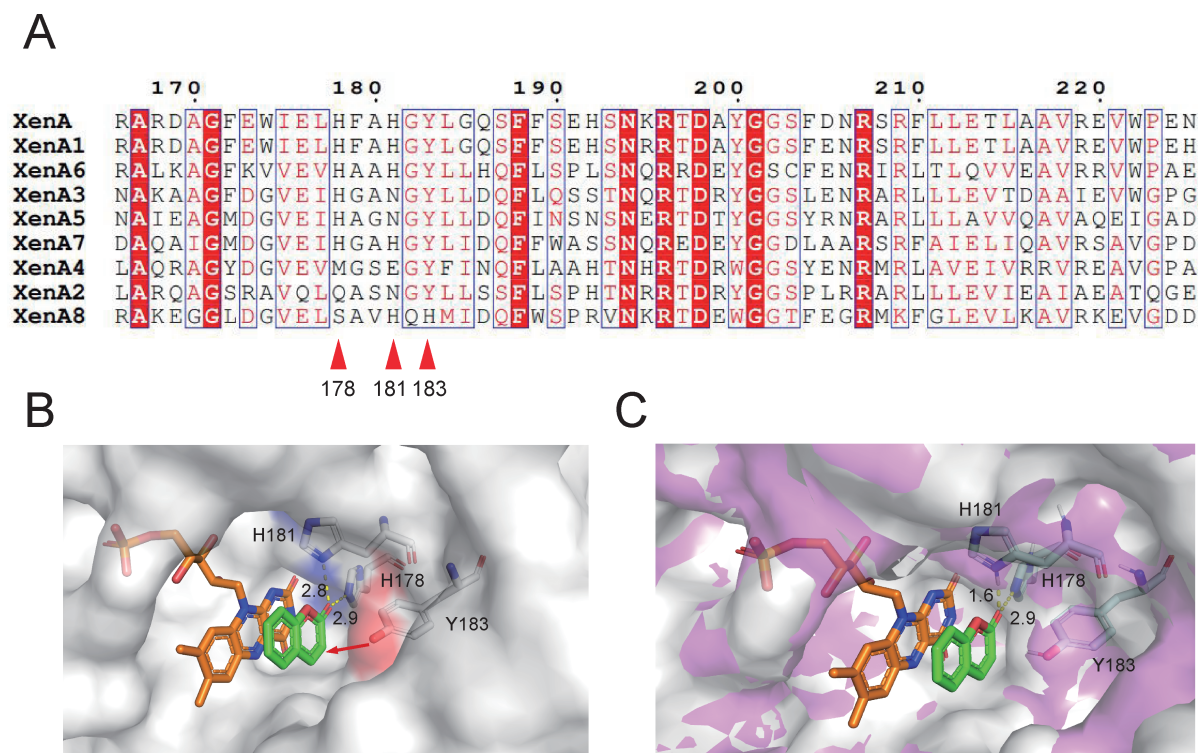


**FIG 8** (A) Sequence alignment of XenA and XenA1-8. The red triangles indicate the residues associated with the substrate binding and catalytic activity. (B) Binding and orientation of COU in the active pocket of XenA (PDB entry 2H90) (B) and XenA1 (C). H178, H181, and Y183 of XenA and residues of XenA1 at the corresponding sites are shown in sticks in the structures; hydrogen-bond interactions between COU and residues are indicated with dotted yellow lines, the distances of which are labeled in angstroms.

gene deletion of *couB1* and *couB2* failed to abolish the ability of strain NyZ480 to grow with COU, which implied that alternative DHC hydrolases possibly exist or the spontaneous hydrolysis rate of DHC is sufficient to maintain an effective catabolic flux *in vivo*.

Despite the presence of genetic redundancy in the first two steps of COU catabolism, gene *couC*, which is responsible for the third transformation step hydroxylating MA to form DHPP, was determined indispensable. The *couC* encoding MA hydroxylase is located 3.2 kb upstream of locus *orf172–orf176* which are highly similar to *mhpBCDEF* encoding conversion of DHPP to acetyl-CoA in 3HPP catabolism pathway (Fig. 1B). In the two catabolic pathways, both 3HPP in *E. coli* K-12 and MA (derived from COU) in strain NyZ480 are firstly converted to the same product DHPP, which is thus completely degraded via the enzymes encoded by the homologous gene cluster, but the enzymes CouC and MhpA (with 26.8% identity) catalyzing the initial hydroxylation which both generates DHPP are distinct. As indicated by the phylogenetic analysis (Fig. 6), CouC is far apart from the MhpA-like 3HPP hydroxylases and clusters with the phenol and dichlorophenol monooxygenases, which is intriguing as MA is more structurally analogous to 3HPP compared to phenol and its chlorinated derivatives. However, analysis of substrate specificity indicated that CouC failed to hydroxylate 4-chlorophenol and 2,4-dichlorophenol and barely had catalytic activity against 2-chlorophenol (Table 2), suggesting that even though CouC may share the same ancestor with chlorophenol monooxygenases, their catalytic specificity became completely different after long-term evolution. On the other hand, CouC hardly catalyzed the conversion of 3HPP, which demonstrated the vital role of the hydroxyl position in determining the hydroxylases for the catalysis of different hydroxyphenylpropionic acids. It is fascinating to notice that the *mhpBCDEF* cluster is highly homologous between the 3HPP degraders and strain NyZ480, whereas the genes encoding the hydroxylation of 3HPP and MA at the previous catabolic step evolve so dramatically to accommodate the catabolism of different substrates. The very

case revealed here is an explicit instance of the convergent evolution in the bacterial catabolism of naturally existing compounds.

## MATERIALS AND METHODS

### Chemicals, strains, plasmids, primers, and culture conditions

All chemicals were purchased from YuanYe Bio-Technology (Shanghai, China), except for MA [Macklin Biochemical Co., Ltd. (Shanghai, China)] and DHPP [Amatek Scientific Co., Ltd. (Zhangjiagang, China)]. Purity of all chemicals is over 97%. Table 3 incorporates all the bacterial strains and plasmids used in this study. Primers used in this study are listed in Table 4. *Pseudomonas* strains were cultured at 30°C in lysogeny broth (LB) or in minimal medium (MM) prepared as previously reported (45), and *E. coli* strains were

TABLE 3 Bacterial strains and plasmids used in this study

Strain or plasmid	Description and characteristics	Source
<b>Strains</b>		
<i>Pseudomonas</i> sp.		
NyZ480	Coumarin degrader	(45)
NyZ480Δ <i>couC</i>	Mutant of strain NyZ480 with the deletion of <i>couC</i>	This study
NyZ480Δ <i>xenA1</i>	Mutant of strain NyZ480 with the deletion of <i>xenA1</i>	This study
NyZ480Δ <i>couB1</i>	Mutant of strain NyZ480 with the deletion of <i>couB1</i>	This study
NyZ480Δ <i>couB2</i>	Mutant of strain NyZ480 with the deletion of <i>couB2</i>	This study
NyZ480Δ <i>couB1ΔcouB2</i>	Mutant of strain NyZ480 with the deletion of both <i>couB1</i> and <i>couB2</i>	This study
NyZ480Δ <i>couC</i> (pMCS- <i>couC</i> )	Mutant NyZ480Δ <i>couC</i> complemented with <i>couC</i>	This study
<i>E. coli</i>		
DH5α	<i>supE44 lacU169(φ80lacZΔM15) hsdR17 recA1 endA1 gyrA96 Δthi relA1</i>	Novagen
BL21(DE3)	<i>F' ompT hsdS<sub>B</sub> (r<sub>B</sub><sup>-</sup> m<sub>B</sub><sup>-</sup>) gal dcm lacY1 (DE3)</i>	Novagen
Rosetta(DE3)	<i>F' ompT hsdS<sub>B</sub> (r<sub>B</sub> m<sub>B</sub>) gal dcm (DE3) pRARE (Cm<sup>r</sup>)</i>	Novagen
S17-1 λpir	<i>thi pro hsdR hsdM<sup>+</sup> recA R<sup>-</sup> M<sup>+</sup> RP4-2-Tc::Mu-Km::Tn7</i>	Stock in lab
<b>Plasmids</b>		
pET-28a(+)	IPTG inducible expression vector; Km <sup>r</sup>	Novagen
pET- <i>xenA1</i>	<i>xenA1</i> fragment inserted into pET-28a(+) between <i>NdeI</i> and <i>BamHI</i> ; Km <sup>r</sup>	This study
pET- <i>xenA2</i>	<i>xenA2</i> fragment inserted into pET-28a(+) between <i>NdeI</i> and <i>BamHI</i> ; Km <sup>r</sup>	This study
pET- <i>xenA3</i>	<i>xenA3</i> fragment inserted into pET-28a(+) between <i>NdeI</i> and <i>BamHI</i> ; Km <sup>r</sup>	This study
pET- <i>xenA4</i>	<i>xenA4</i> fragment inserted into pET-28a(+) between <i>NdeI</i> and <i>BamHI</i> ; Km <sup>r</sup>	This study
pET- <i>xenA5</i>	<i>xenA5</i> fragment inserted into pET-28a(+) between <i>NdeI</i> and <i>BamHI</i> ; Km <sup>r</sup>	This study
pET- <i>xenA6</i>	<i>xenA6</i> fragment inserted into pET-28a(+) between <i>NdeI</i> and <i>BamHI</i> ; Km <sup>r</sup>	This study
pET- <i>xenA7</i>	<i>xenA7</i> fragment inserted into pET-28a(+) between <i>NdeI</i> and <i>BamHI</i> ; Km <sup>r</sup>	This study
pET- <i>xenA8</i>	<i>xenA8</i> fragment inserted into pET-28a(+) between <i>NdeI</i> and <i>BamHI</i> ; Km <sup>r</sup>	This study
pET- <i>couB1</i>	<i>couB1</i> fragment inserted into pET-28a(+) between <i>NdeI</i> and <i>BamHI</i> ; Km <sup>r</sup>	This study
pET- <i>couB2</i>	<i>couB2</i> fragment inserted into pET-28a(+) between <i>NdeI</i> and <i>BamHI</i> ; Km <sup>r</sup>	This study
pET- <i>couC</i>	<i>couC</i> fragment inserted into pET-28a(+) between <i>NdeI</i> and <i>BamHI</i> ; Km <sup>r</sup>	This study
pBBR1MCS-2	Broad-host-range expression vector; Km <sup>r</sup>	This study
pMCS- <i>couC</i>	<i>couC</i> fragment inserted into pBBR1MCS-2 between <i>KpnI</i> and <i>HindIII</i> ; Km <sup>r</sup>	This study
pK18mobsacB	Gene deletion vector, Km <sup>r</sup> , <i>Mob<sup>+</sup></i> , <i>sacB<sup>+</sup></i>	(59)
pK-Δ <i>xenA1</i>	Upstream and downstream fragments of <i>xenA1</i> fused and inserted into pK18mobsacB between <i>EcoRI</i> and <i>BamHI</i> ; Km <sup>r</sup>	This study
pK-Δ <i>couB1</i>	Upstream and downstream fragments of <i>couB1</i> fused and inserted into pK18mobsacB between <i>EcoRI</i> and <i>BamHI</i> ; Km <sup>r</sup>	This study
pK-Δ <i>couB2</i>	Upstream and downstream fragments of <i>couB2</i> fused and inserted into pK18mobsacB between <i>EcoRI</i> and <i>BamHI</i> ; Km <sup>r</sup>	This study
pK-Δ <i>couC</i>	Upstream and downstream fragments of <i>couC</i> fused and inserted into pK18mobsacB between <i>EcoRI</i> and <i>BamHI</i> ; Km <sup>r</sup>	This study

cultured at 37°C in LB. Antibiotics (100 µg/mL ampicillin, 50 µg/mL kanamycin) were added into culture medium when needed.

### Identification of candidate genes and phylogenetic analysis

BLASTP v2.12.0+ was employed to search for candidate genes involved in the catabolism of COU in strain NyZ480, amino acid sequences of characterized enzymes were used as queries, and E-value of the program was set as 1e-20. For phylogenetic analysis, amino acid sequences of interest were recruited. Firstly, sequence alignment was conducted with Muscle v5.1 (60), phylogenetic trees were then constructed by the maximum likelihood method using RAxML-NG (61), and 1,000 bootstrap replicates were used. Visualization was finally completed by iTOL (62).

**TABLE 4** Primers used in this study

Primer	Sequence (5'→3')	Purpose
XenA1-F	CGCGCGGCAGCCATATGATGTCCGCGCTGTTCTGA	Amplification of <i>xenA1</i> for expression in pET-28a(+)
XenA1-R	GCTCGAATTCGGATCCTCAGCGATAGCGCTCGAGC	
XenA2-F	CGCGCGGCAGCCATATGATGACTTCGGGTATCCGCT	Amplification of <i>xenA2</i> for expression in pET-28a(+)
XenA2-R	GCTCGAATTCGGATCCTTAGTCATATCGAATCGAATCGGGCC	
XenA3-F	CGCGCGGCAGCCATATGATGACCACCCTTTTCGATCCGA	Amplification of <i>xenA3</i> for expression in pET-28a(+)
XenA3-R	GCTCGAATTCGGATCCTTACATCCGCGGATAGTCGATGT	
XenA4-F	CGCGCGGCAGCCATATGATGGGGAACCGTTTCATGGC	Amplification of <i>xenA4</i> for expression in pET-28a(+)
XenA4-R	GCTCGAATTCGGATCCTCAAAGCTCCGCCGCCA	
XenA5-F	CGCGCGGCAGCCATATGATGACCAGTAATCTGTTCAATCTATTTCGC	Amplification of <i>xenA5</i> for expression in pET-28a(+)
XenA5-R	GCTCGAATTCGGATCCTTACGGGTGAGTCGGATAGTCGAT	
XenA6-F	CGCGCGGCAGCCATATGATGAGCCTGCTGCTCGAG	Amplification of <i>xenA6</i> for expression in pET-28a(+)
XenA6-R	GCTCGAATTCGGATCCTAATCCCGCAAATCCGATTCGT	
XenA7-F	CGCGCGGCAGCCATATGATGTCAACCAACCCGCTGT	Amplification of <i>xenA7</i> for expression in pET-28a(+)
XenA7-R	GCTCGAATTCGGATCCTCAAGCCAGGGTCGACAATGC	
XenA8-F	CGCGCGGCAGCCATATGATGGCATTCAAGCAATGTTCC	Amplification of <i>xenA8</i> for expression in pET-28a(+)
XenA8-R	GCTCGAATTCGGATCCTCAGAAGTCTTGACAGGGC	
CouB1-F	CGCGCGGCAGCCATATGATGAGCTACGTAACAACCAAAGACG	Amplification of <i>couB1</i> for expression in pET-28a(+)
CouB1-R	GCTCGAATTCGGATCCTCAGCTTTGGATGAACGCCAG	
CouB2-F	CGCGCGGCAGCCATATGATGAGCACACTCGTACCC	Amplification of <i>couB2</i> for expression in pET-28a(+)
CouB2-R	GCTCGAATTCGGATCCTCAGCGCTGCAGGAACG	
CouC-F	CGCGCGGCAGCCATATGATGACTACCTCCACTAGCTTCGA	Amplification of <i>couC</i> for expression in pET-28a(+)
CouC-R	GCTCGAATTCGGATCCTTAACCGAGGACGCTTTGGAGC	
XenA1-up-F	CCATGATTACGAATTCGAGATCCAGGGCGGC	Amplification of the 750 bp upstream fragment of <i>xenA1</i> for gene deletion
XenA1-up-R	GTCTGTCCAAGCGGCCCTTTTCGCG	
XenA1-down-F	AGGGCCGCTTGGACAGACTCCAAGGGTTAAACG	Amplification of the 750 bp downstream fragment of <i>xenA1</i> for gene deletion
XenA1-down-R	CGACTCTAGAGGATCGGAGAAGGTCCGCGACCC	
CouB1-up-F	CGACTCTAGAGGATCGCTTTCCCGCGCGCG	Amplification of the 750 bp upstream fragment of <i>couB1</i> for gene deletion
CouB1-up-R	GCCGCCACGGGTTGTTTCTCCTCCGTAGGGG	
CouB1-down-F	GAAACAACCCGTGGCGGCCCTCG	Amplification of the 750 bp downstream fragment of <i>couB1</i> for gene deletion
CouB1-down-R	CCATGATTACGAATTCGATTTCATGGATACCGTTGGC	
CouB2-up-F	CGACTCTAGAGGATCGTCCGATGCGTTTTTCAGC	Amplification of the 750 bp upstream fragment of <i>couB2</i> for gene deletion
CouB2-up-R	GATACCGACAGGGCGGGGCCGC	
CouB2-down-F	CCATGATTACGAATTCCTACAACGCCCTCACCG	Amplification of the 750 bp downstream fragment of <i>couB2</i> for gene deletion
CouB2-down-R	GCCCCGCTGTGGTATCTCCTTGAAAGTCTGCAG	
CouC-up-F	CGACTCTAGAGGATCCGTGCTCGGCCAGTGG	Amplification of the 750 bp upstream fragment of <i>couC</i> for gene deletion
CouC-up-R	CCTGGAGAATAAGAAGCATTTCCTCAAAGGCCCGG	
CouC-down-F	CCTTTGAGGAAATGCTTCTTATTCTCCAGGCATTACATAGTATGCT	Amplification of the 750 bp downstream fragment of <i>couC</i> for gene deletion
CouC-down-R	CCATGATTACGAATTCGGAAGGCACATTGAGCT	
CouC-mcs-F	GGGAACAAAAGCTGGATGACTACCTCCACTAGCTTCGA	Amplification of <i>couC</i> for complementation
CouC-mcs-R	ATTCGATATCAAGCTTTAACCGAGGACGCTTTGGAGC	



## Structural prediction and molecular docking

3D structures of XenA1, XenA3, XenA5, XenA6, and XenA7 were predicted from their amino acid sequences by AlphaFold 2.1 (63); the derived pLDDT (predicted local distance difference test) values are all over 91.9, indicating high confidence. COU was then docked into the catalytic pocket of the predicted structures with Autodock vina 1.2.3 (64), and results with the lowest affinity value (all less than or equal to  $-7$  kcal/mol) were used for the subsequent analysis. PyMOL 2.1 (<http://www.pymol.org>) was used for the visualization of the binding of COU to the enzymes.

## Construction of plasmids and overexpression of proteins

DNA fragments of interest were amplified using primers listed in Table 4, which were then cloned into linearized plasmids using the ClonExpress MultiS One Step Cloning kit (Vazyme Biotech Co., Ltd., Nanjing, China). For the construction of pK- $\Delta$ couC, pK- $\Delta$ xenA1, pK- $\Delta$ couB1, and pK- $\Delta$ couB2, the upstream fragments of *couC*, *xenA1*, *couB1*, and *couB2* were respectively fused with downstream ones of these genes beforehand and then inserted into digested pK18mobsacB. Plasmids for different purposes were introduced into the corresponding bacterial hosts respectively.

For the overexpression of proteins, *E. coli* strains harboring different plasmids were grown in LB medium to reach an OD<sub>600</sub> of 0.6. Subsequently, the induced expression of genes was triggered by the addition of 0.3 mM IPTG (isopropyl- $\beta$ -D-thiogalactopyranoside) followed by 14-h incubation on a rotary shaker (16°C, 180 rpm).

## Whole cell biotransformation of COU

*E. coli* BL21(DE3) harboring pET-*xenA1*, pET-*xenA2*, pET-*xenA3*, pET-*xenA4*, pET-*xenA5*, pET-*xenA6*, pET-*xenA7*, and pET-*xenA8* were cultured in 50-mL LB medium and induced as described, respectively. Cells were harvested, thoroughly washed with phosphate-buffered saline (PBS) buffer (pH 7.4), and then resuspended in 5-mL MM supplemented with 0.5 mM COU. Incubation of the cell suspensions was carried out on a rotary shaker (30°C, 180 rpm). Sampling was conducted at appropriate time intervals; concentrations of COU, DHC, and MA were measured. Conversion rate of COU by these recombinant enzymes was defined as the amount of COU that was converted to DHC per minute per gram wet weight of bacterial cells at 30°C. HPLC and LC-MS were used as previously described (45) for quantitative and qualitative analyses of different compounds.

## Crude enzyme assays of CouB1 and CouB2

To elucidate the role of CouB1 and CouB2 in the transformation of DHC, pET-28a(+), pET-*couB1*, and pET-*couB2* were transformed into *E. coli* BL21(DE3), respectively. Culture and induction were performed as mentioned above. Thoroughly washed bacterial cells were suspended in 50 mM Tris-HCl buffer (pH 8.0); ultrasonication and subsequent centrifugation (17,000  $\times g$ , 45 min) were performed to obtain crude extracts. Activity of the crude enzyme toward DHC was determined by both HPLC analysis and UV spectrum scanning.

A time course assay for the crude enzymes was performed in 50 mM Tris-HCl buffer (pH 8.0) containing 650-ng crude extracts of CouB1, 10- $\mu$ g crude extracts of CouB2, and 10- $\mu$ g crude extracts of *E. coli* cells harboring pET-28a(+) only, respectively. Control was set by adding an equal volume of Tris-HCl buffer (pH 8.0). A 0.5 mM DHC was added to initiate the reaction. Concentration of DHC and its product MA were measured via HPLC at different sampling points.

As for the enzyme activity test, spectral variation resulted by the transformation of DHC to MA was recorded by a Lambda 25 spectrophotometer (PerkinElmer/Cetus, Norwalk, CT). Crude enzyme activity toward DHC was determined by the decrease of absorbance at 240 nm, which was caused by the dissipation of DHC. The molar extinction coefficient of DHC at 240 nm was determined as 1,964 M<sup>-1</sup> cm<sup>-1</sup> in this study. One unit of crude enzyme activity was defined as the amount of crude enzyme required for the

transformation of 1  $\mu\text{mol}$  DHC in 1 min at 30°C. Specific activity was expressed as units per milligram of protein.

### Purification and characterization of CouC

*couC* was amplified from the genome of strain NyZ480 with the corresponding primers listed in Table 4, which was fused into linearized pET-28a(+) to produce pET-*couC*. The recombinant vector was then introduced into *E. coli* Rosetta (DE3) according to the standard procedure (65). Bacterial cells were cultured and induced as mentioned above. Thoroughly washed bacterial cells were resuspended in 50 mM Tris-HCl buffer (pH 8.0) for ultrasonic fragmentation, and cell extracts were obtained by centrifugation (17,000  $\times g$ , 45 min) and filtered through a 0.45- $\mu\text{m}$  filter membrane. The recombinant His-tagged CouC was eluted with 250 mM imidazole in the Tris-HCl buffer from a 5-mL HisTrap HP column (GE Healthcare). Imidazole contained within the enzyme solution was removed by ultrafiltration. Purity of CouC was analyzed by SDS-PAGE, and protein concentration was determined by Nano-300 (Allsheng Instruments Co., Ltd. Hangzhou, China).

A time course assay was performed to verify the conversion of MA to DHPP catalyzed by purified CouC. The reaction was carried out in 50 mM Tris-HCl buffer (pH 8.0) containing 100-ng CouC, 10  $\mu\text{M}$  FAD, and 200  $\mu\text{M}$  NADH; the reaction was initiated by the addition of 0.1 mM MA. Samples were taken and immediately mixed with an equal volume of acetonitrile to inactivate the enzyme; supernatant was preserved after centrifugation (16,000  $\times g$ , 5 min) and filtration through the 0.22- $\mu\text{m}$  membrane. Concentration of MA and its product DHPP were quantified by HPLC analysis at appropriate time intervals, and LC-MS was employed for the identification of the corresponding chemicals.

Enzyme assay of CouC was conducted in 50 mM Tris-HCl buffer (pH 8.0) containing 80-ng purified CouC, 10  $\mu\text{M}$  FAD, and 200  $\mu\text{M}$  NADH, and the reaction was initiated upon the addition of 100  $\mu\text{M}$  substrate. Relative activity of CouC against all substrates included in Table 2 was determined by the decrease of absorbance at 340 nm, which was caused by the substrate-dependent consumption of the cofactor NADH. The molar extinction coefficient at 340 nm for NADH was 6,220  $\text{M}^{-1} \text{cm}^{-1}$  (66). One unit of enzyme activity was defined as the amount of CouC required for the oxidation of 1  $\mu\text{mol}$  NADH per min at 30°C. Specific activity was defined as above.

### Gene knockout and complementation

The recombinant vectors pK- $\Delta\text{couC}$ , pK- $\Delta\text{xenA1}$ , pK- $\Delta\text{couB1}$ , and pK- $\Delta\text{couB2}$  were respectively introduced into strain NyZ480 via conjugative transfer with the helper *E. coli* S17-1  $\lambda\text{pir}$ . LB plates supplemented with 100  $\mu\text{g}/\text{mL}$  ampicillin and 50  $\mu\text{g}/\text{mL}$  kanamycin were used to screen the single-crossover recombinant strain NyZ480, which was subsequently cultured in LB medium containing the same antibiotics for 12 h at 30°C. Finally, double-crossover recombinants were obtained by plating the culture medium on LB agar containing 10% (wt/vol) sucrose. All gene deletions were further confirmed by sequencing of the PCR products generated from the primers listed in Table 4 for amplification of the flanking fragments upstream and downstream the target genes.

Regarding the complementation of *couC* in mutant NyZ480 $\Delta\text{couC}$ , pMCS-*couC* was generated by inserting *couC* into pBBR1MCS-2. The plasmid pMCS-*couC* was transformed into strain NyZ480 $\Delta\text{couC}$  via electroporation, and the successfully complemented strain was screened on LB plates supplemented with 50  $\mu\text{g}/\text{mL}$  kanamycin. Also, pBBR1MCS-2 without insert was transformed into mutant NyZ480 $\Delta\text{couC}$  to serve as the negative control.

### ACKNOWLEDGMENTS

This work was supported by the National Key R&D Program of China (grant 2021YFA0909500).

## AUTHOR AFFILIATIONS

<sup>1</sup>State Key Laboratory of Microbial Metabolism & School of Life Sciences and Biotechnology, Shanghai Jiao Tong University, Shanghai, China

<sup>2</sup>Joint International Research Laboratory of Metabolic and Developmental Sciences, Shanghai Jiao Tong University, Shanghai, China

## AUTHOR ORCIDs

Yichao Gu  <http://orcid.org/0009-0001-6853-2252>

Tao Li  <http://orcid.org/0000-0002-8255-7798>

Ning-Yi Zhou  <http://orcid.org/0000-0002-0917-5750>

## FUNDING

Funder	Grant(s)	Author(s)
National Key R & D Program of China	2021YFA0909500	Ning-Yi Zhou

## AUTHOR CONTRIBUTIONS

Yichao Gu, Data curation, Formal analysis, Investigation, Methodology, Writing – original draft | Tao Li, Investigation, Methodology, Validation, Writing – review and editing | Ning-Yi Zhou, Conceptualization, Funding acquisition, Project administration, Resources, Supervision, Writing – review and editing

## ADDITIONAL FILES

The following material is available [online](#).

### Supplemental Material

**Supplemental file 1 (AEM01109-23-s0001.docx).** Tables S1 and S2 and Fig. S1 to S5.

## REFERENCES

- Zhalnina K, Louie KB, Hao Z, Mansoori N, da Rocha UN, Shi S, Cho H, Karaoz U, Loqué D, Bowen BP, Firestone MK, Northen TR, Brodie EL. 2018. Dynamic root exudate chemistry and microbial substrate preferences drive patterns in rhizosphere microbial community assembly. *Nat Microbiol* 3:470–480. <https://doi.org/10.1038/s41564-018-0129-3>
- Huang AC, Jiang T, Liu Y-X, Bai Y-C, Reed J, Qu B, Goossens A, Nützmann H-W, Bai Y, Osbourn A. 2019. A specialized metabolic network selectively modulates *Arabidopsis* root microbiota. *Science* 364:eaau6389. <https://doi.org/10.1126/science.aau6389>
- Boisde PM, Meuly WC. 2000. Coumarin, p 647–659. In *Kirk-Othmer encyclopedia of chemical technology*. John Wiley & Sons, Inc. <https://doi.org/10.1002/0471238961.0315211302150919.a01>
- Niro E, Marzaioli R, De Crescenzo S, D'Abrosca B, Castaldi S, Esposito A, Fiorentino A, Rutigliano FA. 2016. Effects of the allelochemical coumarin on plants and soil microbial community. *Soil Biol Biochem* 95:30–39. <https://doi.org/10.1016/j.soilbio.2015.11.028>
- Gutiérrez-Barranquero JA, Reen FJ, McCarthy RR, Dobson ADW, O'Gara F. 2015. Deciphering the role of coumarin as a novel quorum sensing inhibitor suppressing virulence phenotypes in bacterial pathogens. *Appl Microbiol Biotechnol* 99:3303–3316. <https://doi.org/10.1007/s00253-015-6465-9>
- Lee J-H, Kim Y-G, Cho HS, Ryu SY, Cho MH, Lee J. 2014. Coumarins reduce biofilm formation and the virulence of *Escherichia coli* O157:H7. *Phytomedicine* 21:1037–1042. <https://doi.org/10.1016/j.phymed.2014.04.008>
- Yamamoto Y. 2009. Movement of allelopathic compound coumarin from plant residue of sweet vernalgrass (*Anthoxanthum odoratum* L.) to soil. *Grassland Science* 55:36–40. <https://doi.org/10.1111/j.1744-697X.2009.00135.x>
- Lončar M, Jakovljević M, Šubarić D, Pavlič M, Buzjak Služek V, Cindrić I, Molnar M. 2020. Coumarins in food and methods of their determination. *Foods* 9:645. <https://doi.org/10.3390/foods9050645>
- Abraham K, Pfister M, Wöhrlin F, Lampen A. 2011. Relative bioavailability of coumarin from cinnamon and cinnamon-containing foods compared to isolated coumarin: a four-way crossover study in human volunteers. *Mol Nutr Food Res* 55:644–653. <https://doi.org/10.1002/mnfr.201000394>
- Wang Y-H, Avula B, Nanayakkara NPD, Zhao J, Khan IA. 2013. Cassia cinnamon as a source of coumarin in cinnamon-flavored food and food supplements in the United States. *J Agric Food Chem* 61:4470–4476. <https://doi.org/10.1021/jf4005862>
- Woehrlin F, Fry H, Abraham K, Preiss-Weigert A. 2010. Quantification of flavoring constituents in cinnamon: high variation of coumarin in cassia bark from the German retail market and in authentic samples from Indonesia. *J Agric Food Chem* 58:10568–10575. <https://doi.org/10.1021/jf102112p>
- Api AM, Belmonte F, Belsito D, Biserta S, Botelho D, Bruze M, Burton GA, Buschmann J, Cancellieri MA, Dagli ML, Date M, Dekant W, Deodhar C, Fryer AD, Gadhia S, Jones L, Joshi K, Lapczynski A, Lavelle M, Liebler DC, Na M, O'Brien D, Patel A, Penning TM, Ritacco G, Rodriguez-Roperio F, Romine J, Sadekar N, Salvito D, Schultz TW, Sipes IG, Sullivan G, Thakkar Y, Tokura Y, Tsang S. 2019. RIFM fragrance ingredient safety assessment, coumarin, CAS registry number 91-64-5. *Food Chem Toxicol* 130 Suppl 1:110522. <https://doi.org/10.1016/j.fct.2019.05.030>
- Panico A, Serio F, Bagordo F, Grassi T, Idolo A, DE Giorgi M, Guido M, Congedo M, DE Donno A. 2019. Skin safety and health prevention: an overview of chemicals in cosmetic products. *J Prev Med Hyg* 60:E50–E57. <https://doi.org/10.15167/2421-4248/jpmh2019.60.1.1080>
- Nanusha MY, Krauss M, Sørensen BG, Schulze T, Strobel BW, Brack W. 2021. Occurrence of plant secondary metabolite fingerprints in river

- waters from Eastern Jutland, Denmark. *Environ Sci Eur* 33:25. <https://doi.org/10.1186/s12302-021-00464-4>
15. Günthardt BF, Hollender J, Scheringer M, Hungerbühler K, Nanusha MY, Brack W, Bucheli TD. 2021. Aquatic occurrence of phytotoxins in small streams triggered by biogeography, vegetation growth stage, and precipitation. *Sci Total Environ* 798:149128. <https://doi.org/10.1016/j.scitotenv.2021.149128>
  16. Stuart ME, Manamsa K, Talbot JC, Crane EJ. 2011. Emerging contaminants in groundwater. Natural Environment Research Council
  17. Fentem JH, Hammond AH, Garle MJ, Fry JR. 1992. Toxicity of coumarin and various methyl derivatives in cultures of rat hepatocytes and V79 cells. *Toxicol In Vitro* 6:21–25. [https://doi.org/10.1016/0887-2333\(92\)90081-2](https://doi.org/10.1016/0887-2333(92)90081-2)
  18. Ratanasavanh D, Lamiable D, Biour M, Guédès Y, Gersberg M, Leutenegger E, Riché C. 1996. Metabolism and toxicity of coumarin on cultured human, rat, mouse and rabbit hepatocytes. *Fundam Clin Pharmacol* 10:504–510. <https://doi.org/10.1111/j.1472-8206.1996.tb00607.x>
  19. Fentem JH, Fry JR. 1993. Species differences in the metabolism and hepatotoxicity of coumarin. *Comp Biochem Physiol C Comp Pharmacol Toxicol* 104:1–8. [https://doi.org/10.1016/0742-8413\(93\)90102-q](https://doi.org/10.1016/0742-8413(93)90102-q)
  20. Lake BG. 1999. Coumarin metabolism, toxicity and carcinogenicity: relevance for human risk assessment. *Food Chem Toxicol* 37:423–453. [https://doi.org/10.1016/s0278-6915\(99\)00010-1](https://doi.org/10.1016/s0278-6915(99)00010-1)
  21. Loprinzi CL, Kugler JW, Sloan JA, Rooke TW, Quella SK, Novotny P, Mowat RB, Michalak JC, Stella PJ, Levitt R, Tschetter LK, Windschitl H. 1999. Lack of effect of coumarin in women with lymphedema after treatment for breast cancer. *N Engl J Med* 340:346–350. <https://doi.org/10.1056/NEJM199902043400503>
  22. Cox D, O’Kennedy R, Thornes RD. 1989. The rarity of liver toxicity in patients treated with coumarin. *Hum Toxicol* 8:501–506. <https://doi.org/10.1177/096032718900800612>
  23. Cohen AJ. 1979. Critical review of the toxicology of coumarin with special reference to interspecies differences in metabolism and hepatotoxic response and their significance to man. *Food Cosmet Toxicol* 17:277–289. [https://doi.org/10.1016/0015-6264\(79\)90289-x](https://doi.org/10.1016/0015-6264(79)90289-x)
  24. Abraham K, Wöhrlin F, Lindtner O, Heinemeyer G, Lampen A. 2010. Toxicology and risk assessment of coumarin: focus on human data. *Mol Nutr Food Res* 54:228–239. <https://doi.org/10.1002/mnfr.200900281>
  25. Fernandez-Salguero P, Hoffman SM, Cholerton S, Mohrenweiser H, Raunio H, Rautio A, Pelkonen O, Huang JD, Evans WE, Idle JR. 1995. A genetic polymorphism in coumarin 7-hydroxylation: sequence of the human CYP2A genes and identification of variant CYP2A6 alleles. *Am J Hum Genet* 57:651–660.
  26. Hadidi H, Zahlsen K, Idle JR, Cholerton S. 1997. A single amino acid substitution (Leu160His) in cytochrome P450 CYP2A6 causes switching from 7-hydroxylation to 3-hydroxylation of coumarin. *Food Chem Toxicol* 35:903–907. [https://doi.org/10.1016/s0278-6915\(97\)00066-5](https://doi.org/10.1016/s0278-6915(97)00066-5)
  27. Pelkonen O, Rautio A, Raunio H, Pasanen M. 2000. CYP2A6: a human coumarin 7-hydroxylase. *Toxicology* 144:139–147. [https://doi.org/10.1016/s0300-483x\(99\)00200-0](https://doi.org/10.1016/s0300-483x(99)00200-0)
  28. Hsieh CJ, Sun M, Osborne G, Ricker K, Tsai FC, Li K, Tomar R, Phuong J, Schmitz R, Sandy MS. 2019. Cancer hazard identification integrating human variability: the case of coumarin. *Int J Toxicol* 38:501–552. <https://doi.org/10.1177/1091581819884544>
  29. Mizutani T. 2003. PM frequencies of major CYPs in Asians and Caucasians. *Drug Metab Rev* 35:99–106. <https://doi.org/10.1081/dmr-120023681>
  30. Xu P, Huang S-L, Zhu R-H, Han X-M, Zhou H-H. 2002. Phenotypic polymorphism of CYP2A6 activity in a Chinese population. *Eur J Clin Pharmacol* 58:333–337. <https://doi.org/10.1007/s00228-002-0480-3>
  31. Cok I, Aygün Kocabaş N, Cholerton S, Karakaya AE, Sardeş S. 2001. Determination of coumarin metabolism in Turkish population. *Hum Exp Toxicol* 20:179–184. <https://doi.org/10.1191/096032701678766804>
  32. Hadidi H, Irshaid Y, Vågbo CB, Brunsvik A, Cholerton S, Zahlsen K, Idle JR. 1998. Variability of coumarin 7- and 3-hydroxylation in a Jordanian population is suggestive of a functional polymorphism in cytochrome P450 CYP2A6. *Eur J Clin Pharmacol* 54:437–441. <https://doi.org/10.1007/s002280050489>
  33. Rautio A, Kraul H, Kojo A, Salmela E, Pelkonen O. 1992. Interindividual variability of coumarin 7-hydroxylation in healthy volunteers. *Pharmacogenetics* 2:227–233. <https://doi.org/10.1097/00008571-199210000-00005>
  34. Oscarson M, McLellan RA, Gullstén H, Yue Q-Y, Lang MA, Luisa Bernal M, Sinues B, Hirvonen A, Raunio H, Pelkonen O, Ingelman-Sundberg M. 1999. Characterisation and PCR-based detection of a CYP2A6 gene deletion found at a high frequency in a Chinese population. *FEBS Lett* 448:105–110. [https://doi.org/10.1016/S0014-5793\(99\)00359-2](https://doi.org/10.1016/S0014-5793(99)00359-2)
  35. Montanaro D, Lavecchia R, Petrucci E, Zuurro A. 2017. UV-assisted electrochemical degradation of coumarin on boron-doped diamond electrodes. *Chemical Engineering Journal* 323:512–519. <https://doi.org/10.1016/j.cej.2017.04.129>
  36. Dimić DS, Milenković DA, Avdović EH, Nakarada ĐJ, Dimitrić Marković JM, Marković ZS. 2021. Advanced oxidation processes of coumarins by hydroperoxyl radical: an experimental and theoretical study, and ecotoxicology assessment. *Chem Eng J* 424:130331. <https://doi.org/10.1016/j.cej.2021.130331>
  37. Milenković DA, Dimić DS, Avdović EH, Amić AD, Dimitrić Marković JM, Marković ZS. 2020. Advanced oxidation process of coumarins by hydroxyl radical: towards the new mechanism leading to less toxic products. *Chem Eng J* 395:124971. <https://doi.org/10.1016/j.cej.2020.124971>
  38. Görmez Ö, Akay S, Gözmen B, Kayan B, Kalderis D. 2022. Degradation of emerging contaminant coumarin based on anodic oxidation, electro-fenton and subcritical water oxidation processes. *Environ Res* 208:112736. <https://doi.org/10.1016/j.envres.2022.112736>
  39. Huang Y, Sheng B, Yang F, Wang Z, Tang Y, Liu Q, Wang X, Liu J. 2019. Chlorine incorporation into dye degradation by-product (coumarin) in UV/peroxymonosulfate process: a negative case of end-of-pipe treatment. *Chemosphere* 229:374–382. <https://doi.org/10.1016/j.chemosphere.2019.05.024>
  40. Zhao Z, Liu C, Xu Q, Liu Y, Liu X, Yin C, Zhang H, Yan H. 2021. Pathway for biodegrading coumarin by a newly isolated *Pseudomonas* sp. USTB-Z. *World J Microbiol Biotechnol* 37:89. <https://doi.org/10.1007/s11274-021-03055-w>
  41. Nakayama Y, Nonomura S, Tatsumi C. 1973. The metabolism of coumarin by a strain of *Pseudomonas*. *Agr Biol Chem* 37:1423–1437. <https://doi.org/10.1080/00021369.1973.10860852>
  42. Levy CC, Weinstein GD. 1964. Metabolism of coumarin by a microorganism. *Nature* 202:596–597. <https://doi.org/10.1038/202596a0>
  43. Aguirre-Pranzoni C, Orden AA, Bisogno FR, Ardanaz CE, Tonn CE, Kurina-Sanz M. 2011. Coumarin metabolic routes in *Aspergillus* spp. *Fungal Biol* 115:245–252. <https://doi.org/10.1016/j.funbio.2010.12.009>
  44. Bellis DM. 1958. Metabolism of coumarin and related compounds in cultures of *Penicillium* species. *Nature* 182:806–807. <https://doi.org/10.1038/182806a0>
  45. Gu Y, Li T, Yin C-F, Zhou N-Y. 2023. Elucidation of the coumarin degradation by *Pseudomonas* sp. strain NyZ480. *J Hazard Mater* 457:131802. <https://doi.org/10.1016/j.jhazmat.2023.131802>
  46. Xu Y, Zhou N-Y, Kivisaar M. 2020. MhpA is a hydroxylase catalyzing the initial reaction of 3-(3-hydroxyphenyl)propionate catabolism in *Escherichia coli* K-12. *Appl Environ Microbiol* 86:e02385-19. <https://doi.org/10.1128/AEM.02385-19>
  47. Griese JJ, P Jakob R, Schwarzingler S, Dobbek H. 2006. Xenobiotic reductase A in the degradation of quinoline by *Pseudomonas putida* 86: physiological function, structure and mechanism of 8-hydroxycoumarin reduction. *J Mol Biol* 361:140–152. <https://doi.org/10.1016/j.jmb.2006.06.007>
  48. Casellas M, Grifoll M, Bayona JM, Solanas AM. 1997. New metabolites in the degradation of fluorene by *Arthrobacter* sp. strain F101. *Appl Environ Microbiol* 63:819–826. <https://doi.org/10.1128/aem.63.3.819-826.1997>
  49. Kataoka M, Honda K, Shimizu S. 2000. 3,4-dihydrocoumarin hydrolase with haloperoxidase activity from *Acinetobacter calcoaceticus* F46. *Eur J Biochem* 267:3–10. <https://doi.org/10.1046/j.1432-1327.2000.00889.x>
  50. Montersino S, Berkel WJHV. 2013. The flavin monooxygenases, p 51–72. In Hille R, S Miller, B Palfey (ed), *Handbook of flavoproteins*. De Gruyter. <https://doi.org/10.1515/9783110298345>
  51. Zhang J. 2003. Evolution by gene duplication: an update. *Trends Ecol Evol* 18:292–298. [https://doi.org/10.1016/S0169-5347\(03\)00033-8](https://doi.org/10.1016/S0169-5347(03)00033-8)
  52. Deneff VJ, Klappenbach JA, Patrauchan MA, Florizone C, Rodrigues JLM, Tsoi TV, Verstraete W, Eltis LD, Tiedje JM. 2006. Genetic and genomic insights into the role of benzoate-catabolic pathway redundancy in

- Burkholderia xenovorans* LB400. Appl Environ Microbiol 72:585–595. <https://doi.org/10.1128/AEM.72.1.585-595.2006>
53. Frank AM, Chua MJ, Gulvik CA, Buchan A. 2018. Functional redundancy in the hydroxycinnamate catabolism pathways of the salt marsh bacterium *Pigmentiphaga* sp. H8 in 3 - bromo - 4 - hydroxybenzoate - contaminated habitats. Environ Microbiol 24:5123–5138. <https://doi.org/10.1111/1462-2920.16141>
54. Chen K, Xu X, Yang M, Liu T, Liu B, Zhu J, Wang B, Jiang J. 2022. Genetic redundancy of 4 - hydroxybenzoate 3 - hydroxylase genes ensures the catabolic safety of *Pigmentiphaga* sp. H8 in 3 - bromo - 4 - hydroxybenzoate - contaminated habitats. Environ Microbiol 24:5123–5138. <https://doi.org/10.1111/1462-2920.16141>
55. Stassen MJJ, Hsu S-H, Pieterse CMJ, Stringlis IA. 2021. Coumarin communication along the microbiome–root–shoot axis. Trends Plant Sci 26:169–183. <https://doi.org/10.1016/j.tplants.2020.09.008>
56. Robe K, Izquierdo E, Vignols F, Rouached H, Dubos C. 2021. The coumarins: secondary metabolites playing a primary role in plant nutrition and health. Trends Plant Sci. 26:248–259. <https://doi.org/10.1016/j.tplants.2020.10.008>
57. Stringlis IA, Yu K, Feussner K, de Jonge R, Van Bentum S, Van Verk MC, Berendsen RL, Bakker PAHM, Feussner I, Pieterse CMJ. 2018. MYB72-dependent coumarin exudation shapes root microbiome assembly to promote plant health. Proc Natl Acad Sci U S A 115:E5213–E5222. <https://doi.org/10.1073/pnas.1722335115>
58. Lowe-Power TM, Jacobs JM, Ailloud F, Fochs B, Prior P, Allen C, Lindow SE. 2016. Degradation of the plant defense signal salicylic acid protects *Ralstonia solanacearum* from toxicity and enhances virulence on tobacco. mBio 7. <https://doi.org/10.1128/mBio.00656-16>
59. Kovach ME, Elzer PH, Hill DS, Robertson GT, Farris MA, Roop RM 2nd, Peterson KM. 1995. Four new derivatives of the broad-host-range cloning vector pBBR1MCS, carrying different antibiotic-resistance cassettes. Gene 166:175–176. [https://doi.org/10.1016/0378-1119\(95\)00584-1](https://doi.org/10.1016/0378-1119(95)00584-1)
60. Edgar RC. 2022. Muscle5: high-accuracy alignment ensembles enable unbiased assessments of sequence homology and phylogeny. Nat Commun 13:6968. <https://doi.org/10.1038/s41467-022-34630-w>
61. Kozlov AM, Darriba D, Flouri T, Morel B, Stamatakis A, Wren J. 2019. RAxML-NG: a fast, scalable and user-friendly tool for maximum likelihood phylogenetic inference. Bioinformatics 35:4453–4455. <https://doi.org/10.1093/bioinformatics/btz305>
62. Letunic I, Bork P. 2021. Interactive tree of life (iTOL) v5: an online tool for phylogenetic tree display and annotation. Nucleic Acids Res. 49:W293–W296. <https://doi.org/10.1093/nar/gkab301>
63. Jumper J, Evans R, Pritzel A, Green T, Figurnov M, Ronneberger O, Tunyasuvunakool K, Bates R, Židek A, Potapenko A, Bridgland A, Meyer C, Kohl SAA, Ballard AJ, Cowie A, Romera-Paredes B, Nikolov S, Jain R, Adler J, Back T, Petersen S, Reiman D, Clancy E, Zielinski M, Steinegger M, Pacholska M, Berghammer T, Bodenstein S, Silver D, Vinyals O, Senior AW, Kavukcuoglu K, Kohli P, Hassabis D. 2021. Highly accurate protein structure prediction with AlphaFold. Nature 596:583–589. <https://doi.org/10.1038/s41586-021-03819-2>
64. Eberhardt J, Santos-Martins D, Tillack AF, Forli S. 2021. AutoDock Vina 1.2.0: new docking methods, expanded force field, and python bindings. J Chem Inf Model 61:3891–3898. <https://doi.org/10.1021/acs.jcim.1c00203>
65. Mamiatis T, Fritsch EF, Sambrook J, Engel J. 1985. Molecular cloning-a laboratory manual. Cold Spring Harbor Laboratory, New York. <https://doi.org/10.1002/abio.370050118>
66. Zhou N-Y, Fuenmayor SL, Williams PA. 2001. *nag* genes of *Ralstonia* (formerly *Pseudomonas*) sp. strain U2 encoding enzymes for gentisate catabolism. J Bacteriol 183:700–708. <https://doi.org/10.1128/JB.183.2.700-708.2001>